Structural basis of the chiral selectivity of Pseudomonas cepacia lipase

Lang, Dietmar A.; Mannesse, Maurice L.M.; Haas, Gerard H. de; Verheij, Hubertus M.; Dijkstra, Bauke W.

Published in:
European Journal of Biochemistry

DOI:
10.1046/j.1432-1327.1998.2540333.x

Publication date:
1998

Eur. J. Biochem. *254*, 333−340 (1998)

Structural basis of the chiral selectivity of *Pseudomonas cepacia* lipase

Dietmar A. LANG[1], Maurice L. M. MANNESSE[2], Gerard H. DE HAAS[2], Hubertus M. VERHEIJ[2] and Bauke W. DIJKSTRA[1]

[1] BIOSON Research Institute and Laboratory of Biophysical Chemistry, University of Groningen, The Netherlands
[2] Department of Enzymology and Protein Engineering, C.B.L.E., University of Utrecht, The Netherlands

(Received 13 February/1 April 1998) − EJB 98 0222/3

To investigate the enantioselectivity of *Pseudomonas cepacia* lipase, inhibition studies were performed with S_C- and R_C-(R_P,S_P)-1,2-dialkylcarbamoylglycero-3-*O*-*p*-nitrophenyl alkylphosphonates of different alkyl chain lengths. *P. cepacia* lipase was most rapidly inactivated by R_C-(R_P,S_P)-1,2-dioctylcarbamoylglycero-3-*O*-*p*-nitrophenyl octylphosphonate (R_C-trioctyl) with an inactivation half-time of 75 min, while that for the S_C-(R_P,S_P)-1,2-dioctylcarbamoylglycero-3-*O*-*p*-nitrophenyl octyl-phosphonate (S_C-trioctyl) compound was 530 min. X-ray structures were obtained of *P. cepacia* lipase after reaction with R_C-trioctyl to 0.29-nm resolution at pH 4 and covalently modified with R_C-(R_P,S_P)-1,2-dibutylcarbamoylglycero-3-*O*-*p*-nitrophenyl butyl-phosphonate (R_C-tributyl) to 0.175-nm resolution at pH 8.5. The three-dimensional structures reveal that both triacylglycerol analogues had reacted with the active-site Ser87, forming a covalent complex. The bound phosphorus atom shows the same chirality (S_P) in both complexes despite the use of a racemic (R_P,S_P) mixture at the phosphorus atom of the triacylglycerol analogues. In the structure of R_C-tributyl-complexed *P. cepacia* lipase, the diacylglycerol moiety has been lost due to an aging reaction, and only the butyl phosphonate remains visible in the electron density. In the R_C-trioctyl complex the complete inhibitor is clearly defined; it adopts a bent tuning fork conformation. Unambiguously, four binding pockets for the triacylglycerol could be detected: an oxyanion hole and three pockets which accommodate the *sn*-1, *sn*-2, and *sn*-3 fatty acid chains. Van der Waals' interactions are the main forces that keep the radyl groups of the triacylglycerol analogue in position and, in addition, a hydrogen bond to the carbonyl oxygen of the *sn*-2 chain contributes to fixing the position of the inhibitor.

Keywords: crystal structure; transition-state analog; enantioselectivity; lipase; stereospecificity.

Lipases are lipolytic enzymes, which hydrolyze ester bonds of triacylglycerols. However, their substrate specificity is not limited to triacylglycerols. They may also hydrolyze ester bonds of other compounds such as acetyl-arylpropionic acid esters, which are precursors for the nonsteroidal anti-inflammatory agents naproxen and ibuprofen [1]. Because of this broad substrate specificity, and because of their distinct stereopreferences, lipases have found widespread application in the enantioselective synthesis of organic compounds, and in the resolution of racemic mixtures [2].

Over the years crystal structure determinations of various lipases have shown that all lipases contain the α/β hydrolase fold, a structural motif common to a wide variety of hydrolases [3]. Their active sites contain a catalytic triad, Ser-His-Asp/Glu, similar to those of serine proteases [4−6]. Studies with lipases covalently complexed with organosulfates [7], organophosphates [8, 9], or organophosphonates [10−12] demonstrated that, in the presence of lipid-like compounds or organic solvents, their active-site regions may undergo drastic conformational changes, exposing the catalytic residues and the surrounding hydrophobic surface area to the solvent [13].

Although these studies provided insight into the catalytic mechanism of lipases and yielded a proposal for factors determining their enantioselectivity, none of the inhibitors used resembles a natural substrate. Only the recent investigations by Longhi et al. [14] on cutinase, an enzyme which does not show interfacial activation, made use of a triacylglycerol-like inhibitor. Unfortunately, those studies did not reveal any interactions of the inhibitor's fatty acid chains with the protein.

Here we report crystallographic studies of the lipase from *Pseudomonas cepacia*. Structures of the open conformation of this lipase, from crystals grown from organic solvents, have been published recently [15, 16], but no structures are available with bound lipid analogues. We have now investigated the interaction of this enzyme with S_C- and R_C-(R_P,S_P)-1,2-dialkylcarbamoylglycero-3-*O*-*p*-nitrophenyl alkyl-phosphonates, with the alkyl chains consisting of either four carbon atoms (tributyl) or eight carbon atoms (trioctyl). Guided by kinetic studies, the binding mode of the lipase with the R_C-trioctyl and R_C-tributyl compounds was analyzed by X-ray crystallography. For the first time this resulted in a lipase structure with fatty acid chains bound

Correspondence to B. W. Dijkstra, Laboratory of Biophysical Chemistry, University of Groningen, Nijenborgh 4, 9747 AG Groningen, The Netherlands

Fax: +31 50 3634800.

E-mail: bauke@chem.rug.nl

Abbreviations. R_C-tributyl, R_C-(R_P,S_P)-1,2-dibutylcarbamoylglycero-3-*O*-*p*-nitrophenyl butylphosphonate; R_C-trioctyl, R_C-(R_P,S_P)-1,2-dioctylcarbamoylglycero-3-*O*-*p*-nitrophenyl octylphosphonate; S_C-trioctyl, S_C-(R_P,S_P)-2,3-dioctylcarbamoylglycero-1-*O*-*p*-nitrophenyl octylphosphonate.

Enzymes. Lipases (EC 3.1.1), cutinase, *Fusarium solani pisi* esterase, triacylglycerol lipase (EC 3.1.1.3).

Note. Crystallographic coordinates derived here have been deposited with the Brookhaven Protein Data Bank (Upton, USA) under entry codes 4LIP for *P. cepacia* lipase inhibited by R_C-(R_P,S_P)-1,2-dibutylcarbamoylglycero-3-*O*-*p*-nitrophenyl butylphosphonate and 5LIP for *P. cepacia* lipase inhibited by S_C-(R_P,S_P)-2,3-dioctylcarbamoylglycero-1-*O*-*p*-nitrophenyl octylphosphonate.

Table 1. Statistics of data collection and refinement of R_C-trioctyl- and R_C-tributyl-complexed *Pseudomonas cepacia* lipase.

Parameter	Value for complex	
	R_C-trioctyl	R_C-tributyl
Data collection statistics:		
resolution (nm)	5.0−0.29	3.0−0.175
no. observations	22335	140279
no. unique reflections	6515	56937
R-merge (%)	9.2	3.1
R-merge (%) (last shell)	15.8	5.9
mosaicity (°)	0.4	0.3
completeness (%)	98.5	95.3
Refinement:		
resolution range (nm)	2.0−0.29	2.0−0.175
no. reflections	6398	56677
R_{work} (%)	20.7	17.8
R_{free} (%) (no. reflections)	25.2 (606)	20.2 (1721)
Model deviations from ideality:		
bond lengths (nm)	0.0007	0.0005
bond angles (°)	1.5	1.3
B-factors:		
B-value model	group B factors	individual isotropic
Mean *B*-values:		
main chain atoms	6.68 Å^2	8.27 Å^2
side chain atoms	6.70 Å^2	9.61 Å^2
all protein atoms	6.69 Å^2	8.87 Å^2
solvent molecules (no.)	7.49 Å^2 (4)	21.64 Å^2 (563)
ligand (no. atoms)	28.47 Å^2 (38)	5.27 Å^2 (14)
Ca^{2+}	8.66 Å^2	14.68 Å^2

on the enzyme's surface, allowing the factors that are important for this lipase's stereopreferences to be rationalized.

EXPERIMENTAL PROCEDURES

Inhibition experiments. *Pseudomonas cepacia* M-12-33 (Amano Pharmaceuticals Corp. Ltd) lipase was produced from *Pseudomonas* strain ATCC21808 as a host. The enzyme was purified as described previously [17] and its activity was determined spectrophotometrically in the presence of 100 mM Triton X-100, 0.25 mM *p*-nitrophenyl octanoate and 10 mM $CaCl_2$ at pH 8.0 (modified after [18]). Activities were calculated from the increase in absorbance at 400 nm. The inhibitors R_C-(R_P,S_P)-1,2-dibutylcarbamoylglycero-3-*O*-*p*-nitrophenyl butylphosphonate (R_C-tributyl), S_C-(R_P,S_P)-1,2-dioctylcarbamoylglycero-3-*O*-*p*-nitrophenyl octylphosphonate (S_C-trioctyl) and R_C-(R_P,S_P)-1,2-dioctylcarbamoylglycero-3-*O*-*p*-nitrophenyl octylphosphonate (R_C-trioctyl) were synthesised according to Mannesse et al. [19]. They are diastereomeric (S_P,R_P) at phosphorus, but enantiopure at the C2 atom of the glycerol (either R_C or S_C). All inactivation experiments on an analytical scale were done at 25°C. The kinetics of inactivation was followed by incubation of *P. cepacia* lipase (1−5 μM) in 10 mM Tris/HCl pH 8.0 containing 10 mM $CaCl_2$ and 100 mM Triton X-100. The reaction was started by addition of the inhibitor from a concentrated stock solution in acetonitrile to a final concentration of 300 μM. Final acetonitrile concentrations never exceeded 5%. The residual lipase activity was measured by taking aliquots at different times and testing them spectrophotometrically. From the decrease in activity, the half-times of inactivation were determined. The activity measurements of the lipase towards the triacylglycerol analogues (*R*)- and (*S*)-2-decanoylamido-dodecyldecanoate, were performed titrimetrically as described elsewhere [19].

Table 2. Rmsd in C*α* positions of the different *Pseudomonas* lipase models.

Alkyl phosphonate	Rmsd in C*α* position of		
	R_C-tributyl		*P. cepacia* lipase
	model I	model II	
R_C-trioctyl	0.036	0.036	0.043
R_C-tributyl − model I		0.019	0.037
R_C-tributyl − model II			0.041

Preparation of the complexes and crystallization. The lipase-trialkyl complexes were prepared by adding either the R_C-tributyl or the R_C-trioctyl inhibitor dissolved in acetonitrile to the protein solution (8 mg/ml in 20 mM glycine pH 9) in a molar excess of 10:1. After a 90-h incubation at 12°C, the protein/inhibitor solutions were subjected to crystallization screens [20]. Crystals suitable for X-ray analysis grew within 4 weeks using the sitting-drop vapour-diffusion technique.

R_C-Tributyl-inhibited lipase crystals grew from 20% 2-methyl-2,4-pentanediol, 100 mM $CaCl_2$ in 100 mM Tris/HCl pH 8.5 at 12°C. They diffracted to 0.175-nm resolution on the wiggler beamline BW6 of the Max-Planck Institute at DESY in Hamburg using cryo-conditions (90 K). They are monoclinic, spacegroup $P2_1$, with cell dimensions a = 8.404 nm, b = 4.636 nm, c = 8.538 nm and β = 116.53°. This corresponds to a V_M of 0.00225 nm^3/Da [21] assuming 2 molecules/asymmetric unit.

R_C-Trioctyl-inhibited lipase crystals grew from 14% isopropanol, 20 mM $CaCl_2$ in 100 mM sodium acetate pH 4 at 12°C. They diffracted to 0.29-nm resolution on the X-31 beamline of the EMBL outstation at DESY in Hamburg, using cryo-conditions (120 K). They have the monoclinic spacegroup *C*2 with cell dimensions a = 8.873 nm, b = 4.642 nm, c = 8.395 nm and β = 121.23°. This corresponds to a V_M of 0.00224 nm^3/Da [21] assuming 1 molecule/asymmetric unit.

Crystal structure elucidation. The structures were solved by molecular replacement using the *P. cepacia* lipase structure (Protein Data Bank code 3LIP [16]) without water molecules as a starting model. Calculations were done with AMoRe [22]. The structure elucidation was straightforward. For the R_C-trioctyl-inhibited lipase, the highest peak in the cross-rotation function had a correlation coefficient of 0.53 using data between 0.4−1.0-nm resolution. The translation function revealed a shift of the molecule along the *a* and *c* axes of 1/4 of the unit cell lengths. After applying the translation, the overall *R*-factor was 33.1% and the correlation coefficient was 0.69. With this solution an X-PLOR [23] rigid body refinement was done with data between 0.29−0.8-nm resolution which gave an R_{work} of 32.6% and an R_{free} of 33.6%. After positional refinement, bulk solvent correction and manual building of the R_C-trioctyl compound into a difference Fourier density map using the program O [24], the R_{work} and the R_{free} had decreased significantly. The final model includes all 320 amino acids, one Ca^{2+} ion, four water molecules (located inside the protein molecule) and the R_C-trioctyl compound. The final refinement was done with all reflections in the appropriate resolution range giving an overall *R*-value of 21.4% (Table 1).

For R_C-tributyl-inhibited *P. cepacia* lipase, we searched with the monomeric model for a dimer, expecting two solutions 180° apart. The cross-rotation function calculated with data between 0.4−1.0 nm revealed two strong peaks which were related by a

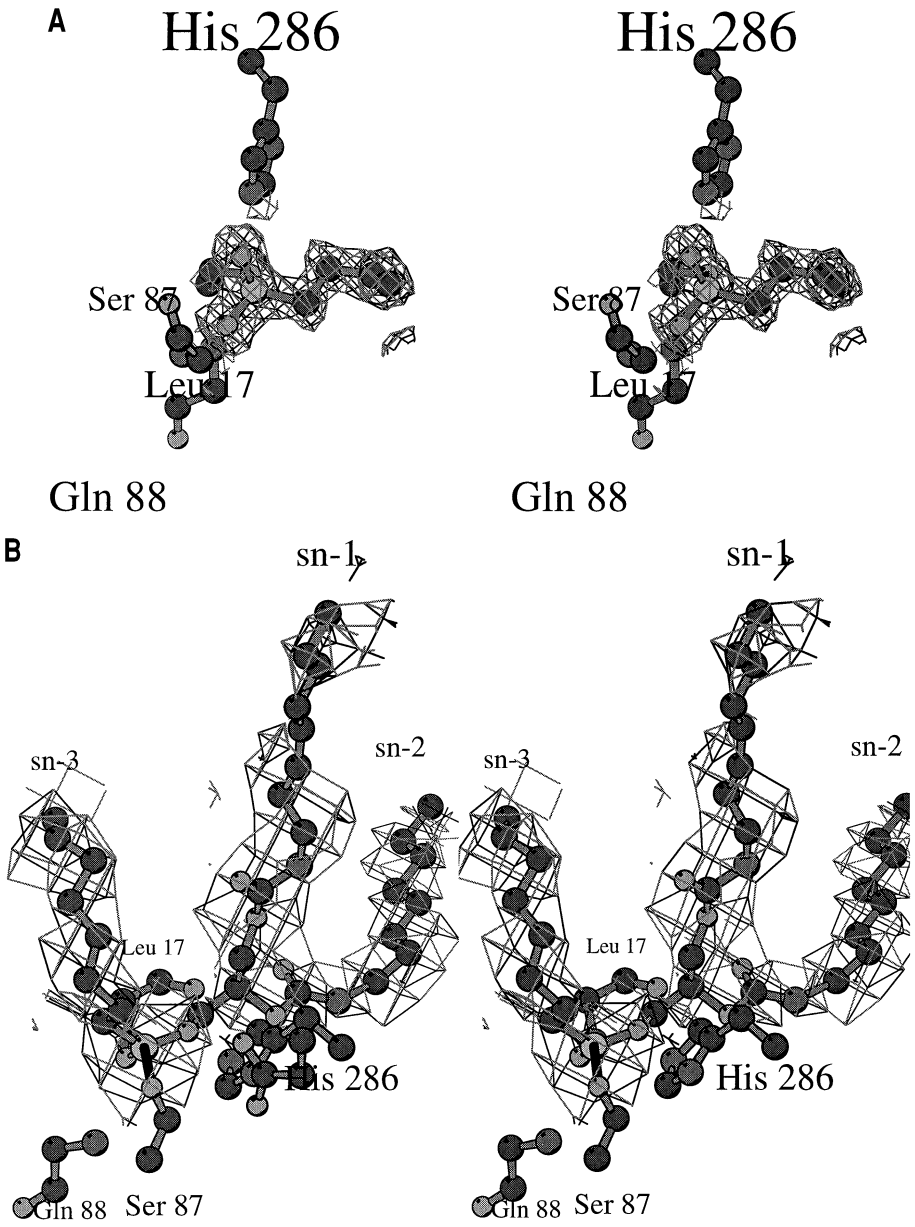

Fig. 1. Stereo-figures of the electron densities of the compounds covalently bound to Ser87 of *P. cepacia* lipase, produced with BOBSCRIPT [42]. (A) *F*o-*F*c omit map of the R_C-tributyl compound, contoured at 2 σ. Only a bound butylphosphonate moiety is visible. (B) 2*F*o-*F*c omit map of R_C-trioctyl compound, contoured at 1 σ. From left to right the *sn*-3, *sn*-1 and *sn*-2 chains are shown.

twofold non-crystallographic symmetry operation parallel to the *b* axis. The translation function found unambiguous peaks for each of the two orientations. Applying the rotation and translation parameters to both independent molecules gave a correlation coefficient of 0.84 and an overall *R*-factor of 32.9%. The refinement was done as described above for the R_C-trioctyl complexed lipase including tight non-crystallographic symmetry restraints for the amino acid regions 2−15, 29−126, 160−217 and 225−320 and individual isotropic *B*-factor refinement. The final model consists of 2×319 amino acid residues, two Ca^{2+} ions, 14 inhibitor atoms and 563 water molecules. The final refinement with all reflections was finished with an *R*-value of 18.2% (Table 1).

RESULTS AND DISCUSSION

Inhibition and X-ray structure determination. The stereoselectivity of *P. cepacia* lipase towards phosphonate triacylglycerol analogues was investigated with two stereoisomers of the trioctyl compound: R_C-trioctyl and S_C-trioctyl. The lipase was most rapidly inactivated by the R_C-trioctyl inhibitor with an observed half-time of 75 min under conditions as described in Experimental Procedures. The corresponding S_C-trioctyl stereoisomer inactivated the lipase with a half-time of 530 min. Since the R_C stereoisomer reacts faster with the enzyme, only the R_C enantiomers of the trioctyl and the tributyl compound were used in the subsequent crystallization experiments. *P. cepacia* lipase, which has an amino acid sequence identical to the *P. cepacia* M-12-33 lipase [25, 26] [and Nakanishi, Y., Kurono, Y., Kolde, Y. & Beppu, T. (1989) European patent no. 0331376], could be complexed and crystallized with R_C-tributyl at pH 8.5 and with R_C-trioctyl at pH 4.0. The statistics of data collection and refinement are summarized in Table 1.

The R_C-tributyl-complexed lipase molecules crystallized as dimers in the asymmetric unit, diffracting to 0.175-nm resolution. After completion of the refinement there was no electron

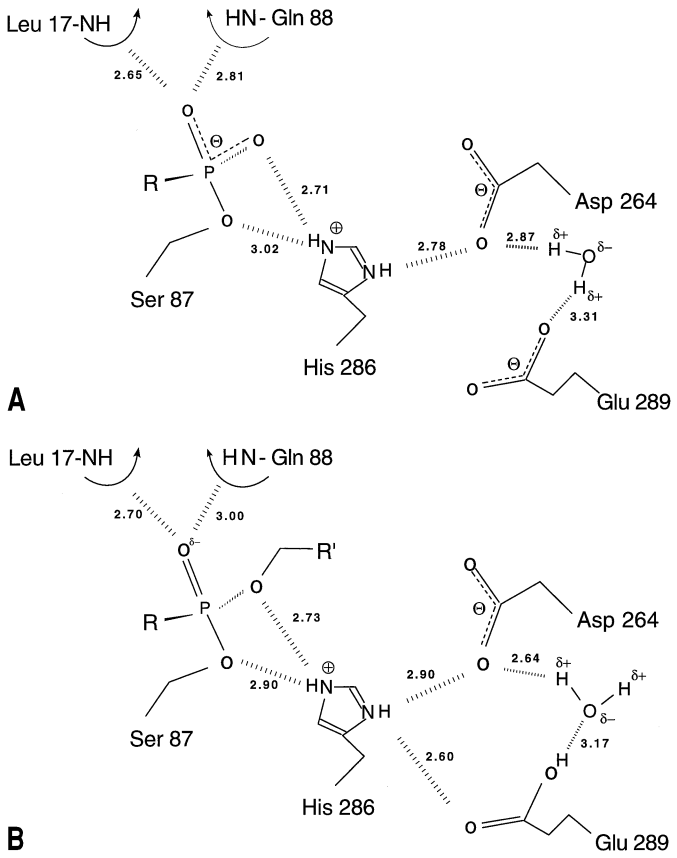

Fig. 2. Schematic representation of the hydrogen bonding pattern of the active-site residues (Ser87, His286, Asp264) and Glu289, with covalently bound acyl and triacylglycerol analogues. The fatty acid part is abbreviated as R, the alcohol part (the diacylglycerol) as R′. (A) Butylphosphonate-complexed *P. cepacia* lipase, crystallized at pH 8.5. (B) R_C-Trioctyl-complexed *P. cepacia* lipase, crystallized at pH 4.0.

density visible for the first amino acid in both molecules and consequently these residues have been left out from the final model. The two molecules differ by 0.019 nm rms in their Cα atom positions (Table 2). In both molecules in the asymmetric unit the inhibitor is covalently bound, but surprisingly only the butyl phosphonate (*sn*-3 moiety) is visible in the electron density maps. Not even weak density is extending from the phosphonate towards the glycerol moiety. This suggests that the glycerol phosphonate ester has been cleaved (Fig. 1A). A nucleophilic substitution of a phosphonate ester bond by the active-site Ser has been observed before in serine proteases [27, 28]. This so-called aging reaction results in the formation of a negatively charged monoester between the active-site Ser and the phosphonate moiety.

The crystals of the R_C-trioctyl-complexed lipase diffracted to 0.29 nm. A solvent-accessible glycine-rich loop (residues 199–202) has a slightly different conformation from that observed in native *P. cepacia* lipase (0.043 nm rms for Cα atoms), probably caused by the glycine flexibility, but the remainder of the protein is unchanged. The complete inhibitor is excellently visible in the difference electron density map (Fig. 1B). The R_C-trioctyl-inhibited structure differs by 0.036 nm in its Cα atom positions from those in the molecules of the R_C-tributyl complex, an rmsd which is slightly higher than the coordinate error of ≈0.02 nm in each structure as estimated from a Luzzati plot [29].

The overall topology of each structure resembles that of the open unliganded form of *P. cepacia* lipase (Protein Data Bank entries 2LIP, 3LIP and 1OIL), previously described in detail [15, 16]. The Ramachandran plots (data not shown) of the native and complexed lipase structures are almost identical, with Ser87 and Leu234 in the disallowed regions, as has been observed for the native lipase as well [15, 16]. The rmsd between all Cα atoms (PDB code 3LIP) and our complexed structures are around 0.04 nm (Table 2), which might be explained by the different temperatures at which the data were collected: native at 298 K and complexed at 90 K and 120 K.

Oxyanion hole and catalytic triad. The R_C-tributyl- and R_C-trioctyl-complexed structures represent the putative transition-state conformation of a substrate molecule bound to the active site. In native *P. cepacia* lipase (Protein Data Bank entry 3LIP) the oxyanion hole has been proposed to be formed by the peptide NH-groups of Gln88 and Leu17 [16]. Indeed, in our complexed structures this site is occupied by one of the phosphonyl oxygen atoms, making hydrogen bonds to the main-chain nitrogen atoms of Gln88 and Leu17, with comparable hydrogen bonding distances in both structures (Fig. 2).

The arrangement of the catalytic residues, Ser87, His286, and Asp264, is similar to that of native *P. cepacia* lipase. However, the Nε2 atom of His286 is also in close contact (≈0.27 nm) with the *O*1 atom of the bound phosphonate inhibitors (Fig. 2). This confirms the hypothesis, put forward by Cygler et al. [30], that the active-site His of the lipase is hydrogen-bonded to both the active-site Ser and the enantio-preferred substrate which, in our case, is the R_C compound. This interaction would facilitate bond cleavage and the departure of the leaving group.

The side chain Oδ1 atom of the catalytic Asp264 is at hydrogen-bonding distance from the Oε1 atom of Glu289 (Fig. 2), as previously described for native *P. cepacia* lipase [16] and the lipase from *Pseudomonas glumae* [31]. This latter lipase has an amino acid sequence identical to that of the *Chromobacterium viscosum* lipase. Because of the much higher resolution of the *C. viscosum* lipase structure (1.6 Å [32]), we have used this lipase instead of *P. glumae* lipase for our structural comparisons. Asp264 in *P. cepacia* lipase makes a further hydrogen bond to one of the internally located water molecules which bridge the catalytic triad residues with the carbonyl oxygens of Gly211, a residue located at C-terminus of β-strand 7 of the central β-sheet [16] and of Val267, one of the last residues of the substrate binding domain (see below). This hydrogen bonding network presumably contributes to the stabilization of the active site of this lipase.

Stereochemistry of the inhibitors. The triacylglycerol inhibitors used are enantiopure at the glycerol backbone C2 atom (R_C), but they are racemic at the phosphorus atom (R_P or S_P). However, the R_C-tributyl- and the R_C-trioctyl-complexed *P. cepacia* lipase structures show that only one phosphorus enantiomer (S_P) is observed. It is generally assumed that the mechanism of phosphonate inhibition of serine hydrolases occurs via an in-line displacement reaction with inversion of configuration at phosphorus [33]. Because the priorities of the substituents at the phosphorus atom as defined by Cahn and co-workers [34] change as a result of the reaction of the phosphonate with serine, the fast-reacting inhibitor must have been the S_P-enantiomer.

The binding pockets. The three-dimensional structure of the R_C-trioctyl inhibitor complexed to *P. cepacia* lipase allows us to describe the different binding pockets (HA, HB and HH, see Figs 3a and 4) and the conformation of this lipid analogue. The lipid has a tuning fork shape, similar to the proposed conformation of a triacylglycerol present at an interface [35]. This conformation is characterized by the glycerol backbone dihedral angles Θ_2 (O5-C2-C3-O3) and Θ_4 (O1-C1-C2-O5) of 89° and 81°, re-

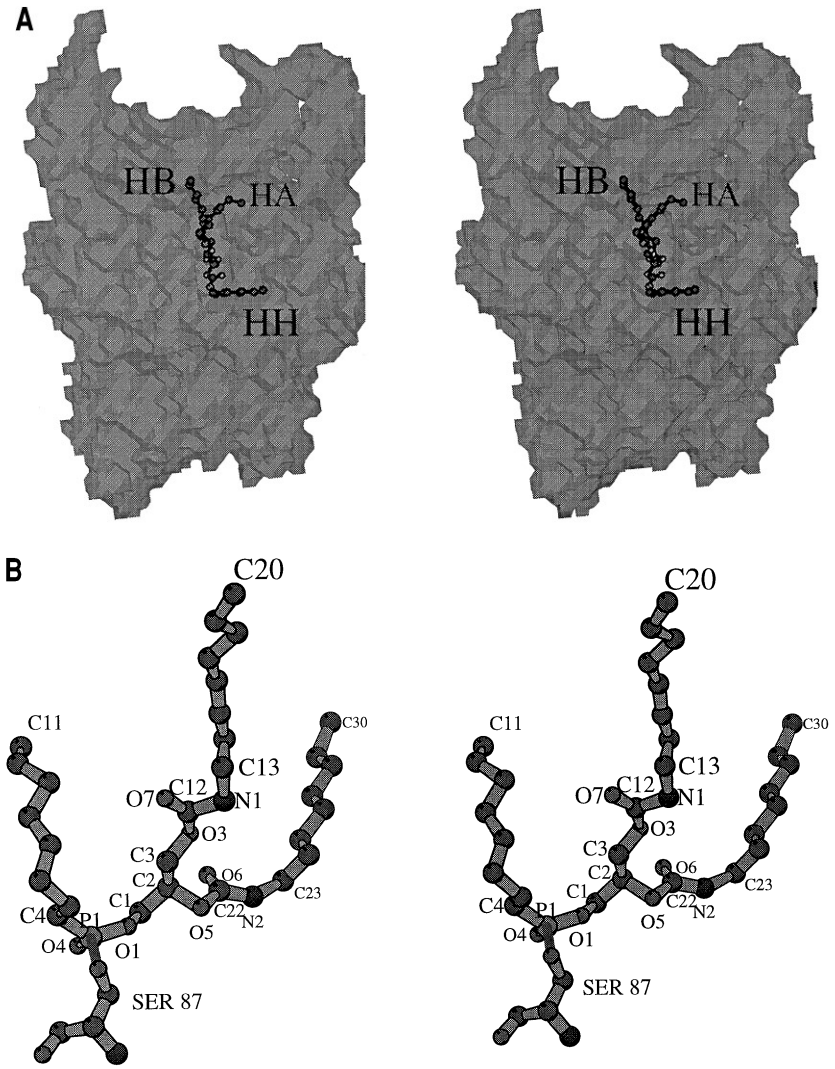

Fig. 3. Stereo-figures of the R_C-trioctyl inhibitor covalently linked to Oγ of Ser87 (produced with the program BOBSCRIPT [42]). (A) Surface map [43] of *P. cepacia* lipase showing the inhibitor bound in a bent tuning-fork conformation. The HA pocket binds the *sn*-3 fatty acid chain, deeply buried in the enzyme's surface, the HH pocket accommodates the *sn*-2 fatty acid chain, and the HB pocket loosely binds the *sn*-1 chain. (B) Close-up of the bound inhibitor with labeled atoms, showing the covalent link between inhibitor and enzyme. Atoms C4−C11 constitute the *sn*-3 chain, atoms N1−C20 the *sn*-1 chain, and atoms N2−C30 the *sn*-2 chain.

spectively [36]. This represents the so called sc/β/sc conformer [35], with the extended octyl chain of the *sn*-2 moiety pointing to the outside (Fig. 3). About 8−10 fatty acid carbon atoms can be accommodated in the pockets. Longer chains probably partly stick into the solvent or micelle.

The binding cleft for the *sn*-3 moiety (HA) is a hydrophobic groove of 0.8×1.0 nm in width. The octyl group of the triacylglycerol analogue fits snugly in this cleft and is bound via van der Waals' interactions (Fig. 4A). Pro113 closes the groove at the C-terminus of the central β sheet and the side-chain atoms of residues Leu17, Phe119, Leu164, Leu167, Val266 and Val267 are in the wall of the cleft. These residues are part of functionally important secondary structure regions: the oxyanion loop (Leu17), helix α6 in the direct neighbourhood of the lid helix α5 (Leu164 and Leu167) and the active-site Asp loop (Val266 and Val267). The *sn*-3 chain of the butylphosphonate (which is the remaining part of the tributyl inhibitor) binds in a very similar way in this groove, with an rmsd of 0.023 nm compared to the equivalent atoms of the octyl chain. This indicates a well conserved mode of *sn*-3 fatty acid binding.

The binding of the *sn*-2 moiety in the HH pocket is also mainly determined by van der Waals interactions (Fig. 4B). The NH group of the carbamoyl function in this chain does not make any specific interactions with the protein. Leu287 and Leu293, both located in the calcium binding loop, make hydrophobic contacts via their Cδ atoms to the carbon atoms of the *sn*-2 octyl chain. In addition, a hydrogen bond connects Oγ of Thr18 to the carbonyl oxygen of the carbamoyl function of this chain. We propose that the *sn*-2 carbonyl oxygen ester of a triacylglycerol molecule can make a comparable hydrogen bond.

The *sn*-1 moiety is bound via hydrophobic interactions to Ala247 and Thr251 in the HB pocket (Fig. 4B), in which a smaller number of van der Waals' interactions is possible. No interactions are made by the NH group of the carbamoyl function.

Enantiomeric selectivity. From the kinetic investigations, we know that the inactivation of *P. cepacia* lipase by the S_C-trioctyl compound is sevenfold slower than the inhibition by the R_C-trioctyl compound. To obtain information about the stereoisomeric discrimination of the enzyme between the S_C- and the R_C-trioctyl compounds, we modelled the S_C-trioctyl compound into the active site of *P. cepacia* lipase by a substituent exchange at the C2 position of the glycerol moiety. The phosphonylalkyl

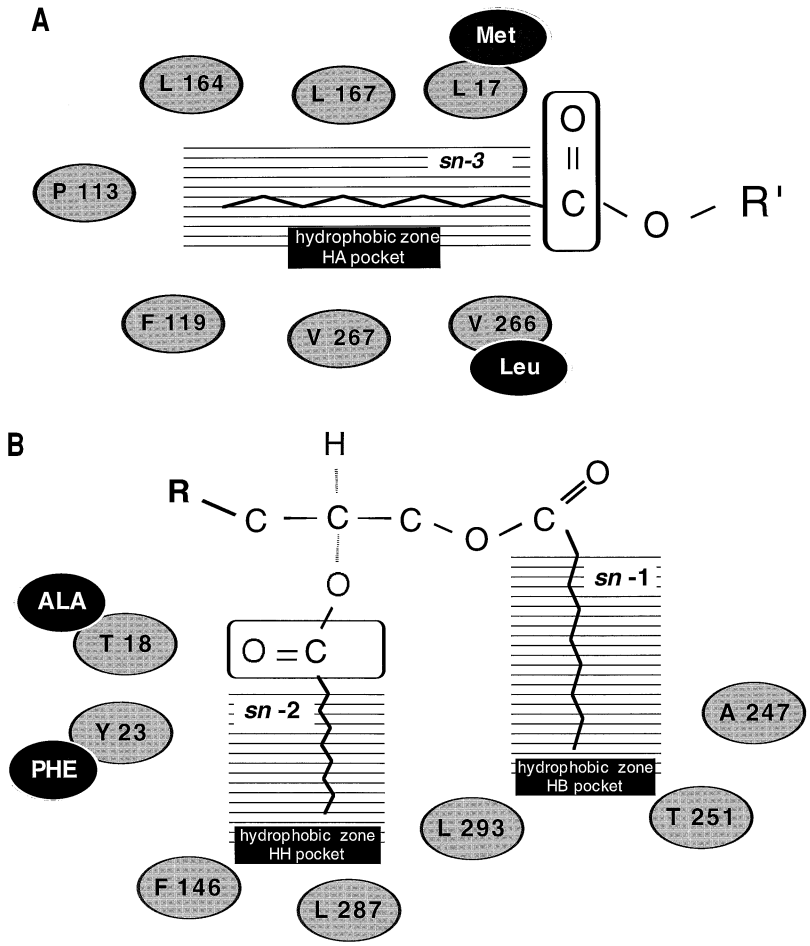

Fig. 4. Schematic representation of the triacylglycerol binding mode in the active site of *P. cepacia* lipase as deduced from the observed binding mode of the R_C-trioctyl inhibitor. The fatty acid part is abbreviated as R, the glycerol part as R′. Residues in *Pseudomonas* spec. involved in binding are indicated. (A) The HA acyl-chain pocket. Leu17 and Val266 are located at the pocket entrance; they are replaced by Met17 and Leu266 (darkened residues) in *P. aeruginosa* lipase [26]. (B) The HB and HH acyl-chain pockets. Thr18 and Tyr23 are replaced by Ala18 and Phe23 in *Chromobacterium viscosum* lipase [26] (darkened residues).

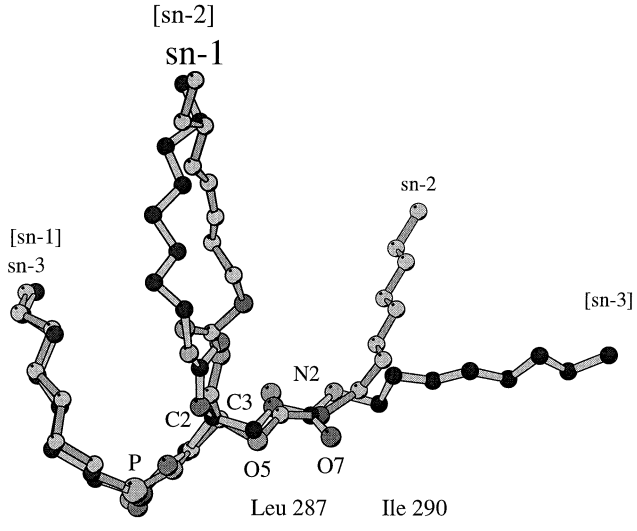

Fig. 5. Superposition of the modeled S_C-trioctyl inhibitor on the R_C-trioctyl compound to demonstrate the ligand substitutions. The R_C-trioctyl compound has its carbon atoms in light grey and bonds in darker grey, the carbon atoms of the S_C-trioctyl model are black, and the bonds are in light grey. The *sn*-nomenclature of the acyl chains is indicated: for the S_C-trioctyl model within square brackets, for the R_C compound without.

chain of the S_C compound remains located in the HA pocket of the enzyme (Fig. 5). According to the stereospecific numbering (*sn*) of glycerol [37], this chain is the *sn*-1 chain in the S_C compound, but the *sn*-3 chain in the R_C compound. The *sn*-3 chain of the S_C-trioctyl compound is now located in the HH pocket, and the *sn*-2 radyl part of this compound is located in the HB pocket (Fig. 5).

In the HH pocket the positions of the O5-C22(O6)-N2 atoms of the R_C-trioctyl compound would be occupied by the C3-O3-C12(O7) atoms of the S_C-trioctyl model. As a result the hydrophilic interaction of the *sn*-2 carbonyl oxygen (O6) with the Oγ1 atom of Thr18 would disappear. We cannot exclude that this interaction might be taken over by an interaction with the 0.36-nm-distant O3 atom. Most important, however, seems to be the orientation of the carbonyl oxygen (O7) in the S_C-trioctyl model, since it would clash with the Cδ2 atom of the hydrophobic side chain of Leu287 (0.24 nm) and the Cδ1 atom of Ile290 (0.27 nm). Consequently, either the carbonyl oxygen (O7) of the compound or the side chains of the appropriate residues must reorient to prevent unfavourable protein−ligand interactions. The presence of such unfavourable interactions might explain the observed preference for the R_C- over the S_C-trioctyl compound. The environment of the *sn*-1 and *sn*-2 substituents near the stereocenter of the R_C compound (or of the *sn*-2 and *sn*-3 chains of the S_C compound) is different: the HB pocket is more hydrophobic, and the HH pocket is more hydrophilic. This ob-

servation underscores the notion by Stadler et al. [38] that substrate engineering at the *sn*-2 position may change the stereoselectivity of lipases.

The results of the modelling experiments described above might explain why *P. cepacia* lipase shows a sevenfold preference for the (*R*)-inhibitor over the (*S*)-inhibitor, which corresponds to an *sn*-3 preference. The stereoselectivity is however dependent on many more factors. For example, Rogalska and co-workers [39] reported a clear *sn*-1 preference for *P. cepacia* lipase acting on trioctanoylglycerol and trioleoylglycerol emulsions. We used the (*R*)- and (*S*)-enantiomers of 2-decanoylamido-1-dodecanoyldecanol, which can be regarded as tridecanoylglycerol analogues containing only one hydrolysable ester bond [19]. We tested these substrates as mixed micelles in the presence of Triton X-100 essentially as described before for cutinase [19]. No stereopreference for either the (*R*)- or the (*S*)-enantiomer was found (data not shown). Thus the stereoselectivity of *P. cepacia* lipase seems to be dependent on the chemical nature and/or the physical state of the substrate, as has been observed before for other lipases [38, 40].

Comparison with homologous lipases. Comparison of the amino acids involved in binding of the different parts of the triacylglycerol analogue reveals important differences between members of the *Pseudomonas* lipase family [26]. Between *P. cepacia* lipase and *P. aeruginosa* lipase [41], Leu17→Met and Val266→Leu substitutions influence the size and the width of the HA pocket, where the *sn*-3 fatty acid chain binds (Fig. 4A). The Val266→Leu substitution is also one of the amino acid differences between *P. cepacia* lipase and *P. glumae* lipases, others being two amino acid substitutions in the HH pocket (Thr18→Ala and Tyr23→Phe) that might reduce the hydrophilicity of this pocket in *P. glumae* lipase and affect the interaction with the substrate's *sn*-2 carbonyl oxygen atom (Fig. 4B).

CONCLUSIONS

The present crystal structures provide valuable information on the factors that are important for the stereoselectivity of *P. cepacia* lipase. A hydrophobic, well defined groove is the binding site for the *sn*-3 fatty acid chain of the substrate. The binding site for the *sn*-2 chain is subdivided into a small hydrophilic patch where, at the bottom of a cleft, the ester bond region is bound and a larger hydrophobic patch towards the surface, where the hydrophobic part of the *sn*-2 fatty acid chain is bound. The *sn*-2 chain is separated from the *sn*-1 acyl chain by residues from the calcium binding loop. The small *sn*-1 binding site is slightly hydrophobic, and has few interactions with the inhibitor. Among the members of the Pseudomonadaceae family the size and/or the ratio between hydrophobicity and hydrophilicity of these *sn*-2 and *sn*-3 binding sites vary, allowing the different regio- and enantio-specificities of these lipases to be rationalized. This result may be helpful for bacterial lipase engineering to improve their industrial applicability in bioconversion reactions.

We thank the co-workers at the European Molecular Biology Laboratory (EMBL) and the Max-Planck Institute in Hamburg for their support with data collection. We thank the European Union for support of the work at EMBL Hamburg through the European Union BIOTECH program (contract number BIO2 CT94-3013) and the Human Capital and Mobility Program Access to Large Installations Project, contract number CHGE-CT93-0040.

REFERENCES

1. Bando, T., Namba, Y. & Shishido, K. (1997) Lipase-mediated asymmetric construction of 2-arylpropionic acids: enantiocontrolled syntheses of *S*-naproxen and *S*-ibuprofen, *Tetrahedron: Asymmetry 8*, 2159−2165.
2. Theil, F. (1995) Lipase-supported synthesis of biologically active compounds, *Chem. Rev. 95*, 2203−2227.
3. Ollis, D. L., Shea, E., Cygler, M., Dijkstra, B., Frolow, F., Franken, S. M., Harel, M., Remington, S. J., Silman, I., Schrag, J., Sussman, J. L., Verschueren, K. H. G. & Goldman, A. (1992) The α/β hydrolase fold, *Protein Eng. 5*, 197−211.
4. Brady, L., Brzozowski, A. M., Derewenda, Z. S., Dodson, E., Dodson, G., Tolley, S., Turkenburg, J. P., Christiansen, L., Huge-Jensen, B., Norskov, L., Thim, L. & Menge, U. (1990) A serine protease triad forms the catalytic centre of a triacylglycerol lipase, *Nature 343*, 767−770.
5. Schrag, J. D., Li, Y., Wu, S. & Cygler, M. (1991) Ser-His-Glu triad forms the catalytic site of the lipase from *Geotrichum candidum*, *Nature 351*, 761−764.
6. Winkler, F. K., D'Arcy, A. & Hunziker, W. (1990) Structure of human pancreatic lipase, *Nature 343*, 771−774.
7. Grochulski, P., Li, Y., Schrag, J. D. & Cygler, M. (1994) Two conformational states of *Candida rugosa* lipase, *Protein Sci. 3*, 82−91.
8. Brzozowski, A. M., Derewenda, U., Derewenda, Z. S., Dodson, G. G., Lawson, D. M., Turkenburg, J. P., Bjorkling, F., Huge-Jensen, B., Patkar, S. A. & Thim, L. (1991) A model for interfacial activation in lipases from the structure of a fungal lipase-inhibitor complex, *Nature 351*, 491−494.
9. Derewenda, U., Brzozowski, A. M., Lawson, D. M. & Derewenda, Z. S. (1992) Catalysis at the interface: the anatomy of a conformational change in a triacylglycerol lipase, *Biochemistry 31*, 1532−1541.
10. Egloff, M.-P., Marguet, F., Buono, G., Verger, R., Cambillau, C. & van Tilbeurgh, H. (1995) The 2.46 Å resolution structure of the pancreatic lipase-colipase complex inhibited by a C11 alkyl phosphonate, *Biochemistry 34*, 2751−2762.
11. Grochulski, P., Li, Y., Schrag, J. D., Bouthillier, F., Smith, P., Harrison, D., Rubin, B. & Cygler, M. (1993) Insights into interfacial activation from an open structure of *Candida rugosa* lipase, *J. Biol. Chem. 268*, 12843−12847.
12. van Tilbeurgh, H., Egloff, M.-P., Martinez, C., Rugani, N., Verger, R. & Cambillau, C. (1993) Interfacial activation of the lipase-procolipase complex by mixed micelles revealed by X-ray crystallography, *Nature 362*, 814−820.
13. Derewenda, Z. S. (1994) Structure and function of lipases, *Adv. Protein Chem. 45*, 1−52.
14. Longhi, S., Mannesse, M., Verheij, H. M., de Haas, G. H., Egmond, M., Knoops-Mouthuy, E. & Cambillau, C. (1997) Crystal structure of cutinase covalently inhibited by a triacylglycerol analogue, *Protein Sci. 6*, 275−286.
15. Kim, K. K., Song, H. K., Shin, D. H., Hwang, K. Y. & Suh, S. W. (1997) The crystal structure of a triacylglycerol lipase from *Pseudomonas cepacia* reveals a highly open conformation in the absence of a bound inhibitor, *Structure 5*, 173−185.
16. Schrag, J. D., Li, Y., Cygler, M., Lang, D., Burgdorf, T., Hecht, H.-J., Schmid, R., Schomburg, D., Rydel, T. J., Oliver, J. D., Strickland, L. C., Dunaway, C. M., Larson, S. B., Day, J. & McPherson, A. (1997) The open conformation of a *Pseudomonas* lipase, *Structure 5*, 187−202.
17. Kordel, M., Hofmann, B., Schomburg, D. & Schmid, R. D. (1991) Extracellular lipase of *Pseudomonas* sp. strain ATCC 21808: purification, characterization, crystallization, and preliminary X-ray diffraction data, *J. Bacteriol. 173*, 4836−4841.
18. Winkler, U. K. & Stuckmann, M. (1979) Glycogen, hyaluronate, and some other polysaccharides greatly enhance the formation of exolipase by *Serratia marcescens*, *J. Bacteriol. 138*, 663−670.
19. Mannesse, M. L. M., Boots, J. W. P., Dijkman, R., Slotboom, A. J., van der Hijden, H. T. W. V., Egmond, M. R., Verheij, H. M. & de Haas, G. H. (1995) Phosphonate analogues of triacylglycerols are potent inhibitors of lipase, *Biochim. Biophys. Acta 1259*, 56−64.
20. Jancarik, J. & Kim, S. H. (1991) Sparse matrix sampling: a screening method for crystallization of proteins, *J. Appl. Crystallogr. 24*, 409−411.
21. Matthews, B. W. (1968) Solvent content of protein crystals, *J. Mol. Biol. 33*, 491−497.

22. Navaza, J. (1994) AMoRe: an automated package for molecular replacement, *Acta Crystallogr. A50*, 157−163.
23. Brünger, A. T. (1991) Crystallographic phasing and refinement of macromolecules, *Curr. Opin. Struct. Biol. 1*, 1016−1022.
24. Jones, T. A., Zou, J. Y., Cowan, S. W. & Kjeldgaard, M. (1991) Improved methods for building protein models in electron density maps and the location of errors in these models, *Acta Crystallogr. A47*, 110−119.
25. Nakanishi, Y., Watanabe, H., Washizu, K., Narahashi, Y. & Kurono, Y. (1991) Cloning, sequencing and regulation of the lipase gene from *Pseudomonas* sp. M-12-33, in *Lipases: structure, mechanism and genetic engineering* (Alberghina, L., Schmid, R. D. & Verger, R., eds) pp. 263−266, VCH, Weinheim.
26. Gilbert, E. J. (1993) *Pseudomonas* lipases: biochemical properties and molecular cloning, *Enzyme Microb. Technol. 15*, 634−645.
27. Bender, M. L. & Wedler, F. C. (1972) Phosphate and carbonate ester 'aging' reactions with α-chymotrypsin, *J. Am. Chem. Soc. 94*, 2101−2109.
28. Bencsura, A., Enyedy, I. & Kovach, I. M. (1995) Origins and diversity of the aging reaction in phosphonate adducts of serine hydrolase enzymes: what characteristics of the active site do they probe? *Biochemistry 34*, 8989−8999.
29. Luzzati, V. (1952) Traitement statistique des erreurs dans la détermination des structures cristallines, *Acta Crystallogr. 5*, 802−810.
30. Cygler, M., Grochulski, P., Kazlauskas, R. J., Schrag, J. D., Bouthillier, F., Rubin, B., Serreqi, A. N. & Gupta, A. K. (1994) A structural basis for the chiral preferences of lipases, *J. Am. Chem. Soc. 116*, 3180−3186.
31. Noble, M. E. M., Cleasby, A., Johnson, L. N., Egmond, M. R. & Frenken, L. G. J. (1993) The crystal structure of triacylglycerol lipase from *Pseudomonas glumae* reveals a partially redundant catalytic aspartate, *FEBS Lett. 331*, 123−128.
32. Lang, D., Hofmann, B., Haalck, L., Hecht, H.-J., Spener, F., Schmid, R. D. & Schomburg, D. (1996) Crystal structure of a bacterial lipase from *Chromobacterium viscosum* ATCC 6918 refined at 1.6 Å resolution, *J. Mol. Biol. 259*, 704−717.
33. Kovach, I. M., Huhta, D. & Baptist, S. (1991) Active site interactions in hydrated trypsin organophosphate adducts: a yeti molecular mechanics study, *J. Mol. Struct. 226*, 99−110.
34. Cahn, R. S., Ingold, C. & Prelog, V. (1966) Spezifikation der molekularen chiralität, *Angew. Chem. 78*, 413−447.
35. Pascher, I. (1996) The different conformations of the glycerol region of crystalline acylglycerols, *Curr. Opin. Struct. Biol. 6*, 439−448.
36. Sundaralingam, M. (1972) Molecular structures and conformations of the phospholipids and sphingomyelins, *Ann. N.Y. Acad. Sci. 195*, 324−355.
37. IUPAC-IUB Commission on Biochemical Nomenclature (1977) The nomenclature of lipids, *Eur. J. Biochem. 79*, 11−21.
38. Stadler, P., Kovac, A., Haalck, L., Spener, F. & Paltauf, F. (1995) Stereoselectivity of microbial lipases. The substitution at position *sn*-2 of triacylglycerol analogs influences the stereoselectivity of different microbial lipases, *Eur. J. Biochem. 227*, 335−343.
39. Rogalska, E., Cudrey, C., Ferrato, F. & Verger, R. (1993) Stereoselective hydrolysis of triacylglycerols by animal and microbial lipases, *Chirality 5*, 24−30.
40. Zandonella, G., Haalck, L., Spener, F., Faber, K., Paltauf, F. & Hermetter, A. (1995) Inversion of lipase stereospecificity for fluorogenic alkyldiacyl glycerols. Effect of substrate solubilization, *Eur. J. Biochem. 231*, 50−55.
41. Jaeger, K.-E., Ransac, S., Dijkstra, B. W., Colson, C., van Heuvel, M. & Misset, O. (1994) Bacterial lipases, *FEMS Microbiol. Rev. 15*, 29−63.
42. Esnouf, R. M. (1997) An extensively modified version of Molscript that includes greatly enhanced coloring capabilities, *J. Mol. Graph. Modell. 15*, 133−138.
43. Connolly, M. L. (1983) Solvent-accessible surfaces of proteins and nucleic acids, *Science 221*, 709−711.